

Functionalization of Metallabenzenes through Nucleophilic Aromatic Substitution of Hydrogen

George R. Clark, Lauren A. Ferguson, Amy E. McIntosh, Tilo Söhnel, and L. James Wright*

Department of Chemistry, The University of Auckland, Private Bag 92019, Auckland, New Zealand

Received June 15, 2010; E-mail: lj.wright@auckland.ac.nz

Abstract: The cationic metallabenzenes $[\text{Ir}(\text{C}_5\text{H}_4\{\text{SMe-1}\})(\kappa^2\text{-S}_2\text{CNEt}_2)(\text{PPh}_3)_2]\text{PF}_6$ (**1**) and $[\text{Os}(\text{C}_5\text{H}_4\{\text{SMe-1}\})(\text{CO})_2(\text{PPh}_3)_2][\text{CF}_3\text{SO}_3]$ (**2**) undergo regioselective nucleophilic aromatic substitution of hydrogen at the metallabenzene ring position γ to the metal in a two-step process that first involves treatment with appropriate nucleophiles and then oxidation. Thus, reaction between compound **1** and NaBH_4 , MeLi , or NaOEt gives the corresponding neutral iridacyclohexa-1,4-diene complexes $\text{Ir}(\text{C}_5\text{H}_3\{\text{SMe-1}\}\{\text{H-3}\}\{\text{Nu-3}\})(\kappa^2\text{-S}_2\text{CNEt}_2)(\text{PPh}_3)_2$ ($\text{Nu} = \text{H}$ (**3**), Me (**4**), OEt (**5**)). Similarly, reaction between **2** and NaBH_4 or MeLi gives the corresponding osmacyclohexa-1,4-diene complexes $\text{Os}(\text{C}_5\text{H}_3\{\text{SMe-1}\}\{\text{H-3}\}\{\text{Nu-3}\})(\text{CO})_2(\text{PPh}_3)_2$ ($\text{Nu} = \text{H}$ (**8**), Me (**9**)). The metallacyclohexa-1,4-diene rings in all these compounds are rearomatized on treatment with the oxidizing agent O_2 , CuCl_2 , or 2,3-dichloro-5,6-dicyano-1,4-benzoquinone (DDQ). Accordingly, the cationic metallabenzene **1** or **2** is returned after reaction between **3** and DDQ/ NEt_4PF_6 or between **8** and DDQ/ NaO_3SCF_3 , respectively. The substituted cationic iridabenzene $[\text{Ir}(\text{C}_5\text{H}_3\{\text{SMe-1}\}\{\text{Me-3}\})(\kappa^2\text{-S}_2\text{CNEt}_2)(\text{PPh}_3)_2]\text{PF}_6$ (**6**) or $[\text{Ir}(\text{C}_5\text{H}_4\{\text{SMe-1}\}\{\text{OEt-3}\})(\kappa^2\text{-S}_2\text{CNEt}_2)(\text{PPh}_3)_2]\text{PF}_6$ (**7**) is produced in a similar manner through reaction between **4** or **5**, respectively, and DDQ/ NEt_4PF_6 , and the substituted cationic osmabenzene $[\text{Os}(\text{C}_5\text{H}_3\{\text{SMe-1}\}\{\text{Me-3}\})(\text{CO})_2(\text{PPh}_3)_2]\text{Cl}$ (**10**) is formed in good yield on treatment of **9** with CuCl_2 . The starting cationic iridabenzene **1** is conveniently prepared by treatment of the neutral iridabenzene $\text{Ir}(\text{C}_5\text{H}_4\{\text{SMe-1}\})\text{Cl}_2(\text{PPh}_3)_2$ with $\text{NaS}_2\text{CNEt}_2$ and NEt_4PF_6 , and the related starting cationic osmabenzene **2** is obtained by treatment of $\text{Os}(\text{C}_5\text{H}_4\{\text{S-1}\})(\text{CO})(\text{PPh}_3)_2$ with $\text{CF}_3\text{SO}_3\text{CH}_3$ and CO . The stepwise transformations of **1** into **6** or **7** as well as **2** into **10** provide the first examples in metallabenzene chemistry of regioselective nucleophilic aromatic substitutions of hydrogen by external nucleophiles. DFT calculations have been used to rationalize the preferred sites for nucleophilic attack at the metallabenzene rings of **1** and **2**. The crystal structures of **1**, **3**, **6**, and **7** have been obtained.

Introduction

The study of metallabenzenes has continued to attract growing interest over the past decade, and some patterns in the reactivity of these species are beginning to emerge.^{1–4} Reported reactions involving metallabenzenes can be divided into two broad classes, those that have direct counterparts in benzene chemistry and those that do not. This division has been alluded to by a number of authors, often in the context of discussions relating to aromaticity.^{1,2} Metallabenzene reactions that have no counterparts in benzene chemistry include cycloadditions,^{5–7} C–C coupling to form cyclopentadienyl ligands,^{8–10} and ancillary ligand substitutions.^{1,2} The direct involvement of the metal atom

is common to all these reactions. Metallabenzene reactions that have a direct correspondence to classic benzene chemistry are still very restricted in number. Included in this class are the electrophilic aromatic substitution reactions of osma¹¹ and iridabenzene¹² and the formation of η^6 -complexes through the interaction of the metal–ligand fragment “ $\text{Mo}(\text{CO})_3$ ” with irida^{13,14} and platinabenzene.¹⁵ Other relevant isolated examples include the formation of analogs of Jackson–Meisenheimer complexes through the addition of OH^- ,¹⁶ OMe^- ,¹⁷ or phos-

- (1) Bleeke, J. R. *Chem. Rev.* **2001**, *101*, 1205–1227.
- (2) Landorf, C. W.; Haley, M. M. *Angew. Chem., Int. Ed.* **2006**, *45*, 3914–3936.
- (3) Wright, L. J. *Dalton Trans.* **2006**, 1821–1827.
- (4) He, G.; Xia, H.; Jia, G. *Chin. Sci. Bull.* **2004**, *49*, 1543–1553.
- (5) Bleeke, J. R.; Behm, R.; Xie, Y.-F.; Clayton, T. W., Jr.; Robinson, K. D. *J. Am. Chem. Soc.* **1994**, *116*, 4093–4094.
- (6) Iron, M. A.; Martin, J. M. L.; van der Boom, M. E. *J. Am. Chem. Soc.* **2003**, *125*, 11702–11709.
- (7) Iron, M. A.; Martin, J. M. L.; van der Boom, M. E. *Chem. Commun.* **2003**, 132–133.
- (8) Wu, H.-P.; Weakley, T. J. R.; Haley, M. M. *Chem.—Eur. J.* **2005**, *11*, 1191–1200.

- (9) Iron, M. A.; Lucassen, A. C. B.; Cohen, H.; van der Boom, M. E.; Martin, J. M. L. *J. Am. Chem. Soc.* **2004**, *126*, 11699–11710.
- (10) Iron, M. A.; Martin, J. M. L.; van der Boom, M. E. *J. Am. Chem. Soc.* **2003**, *125*, 13020–13021.
- (11) Rickard, C. E. F.; Roper, W. R.; Woodgate, S. D.; Wright, L. J. *Angew. Chem., Int. Ed.* **2000**, *39*, 750–752.
- (12) Clark, G. R.; Johns, P. M.; Roper, W. R.; Wright, L. J. *Organometallics* **2008**, *27*, 451–454.
- (13) Bleeke, J. R.; Xie, Y. F.; Bass, L. A.; Chiang, M. Y. *J. Am. Chem. Soc.* **1991**, *113*, 4703–4704.
- (14) Bleeke, J. R.; Bass, L. A.; Xie, Y. F.; Chiang, M. Y. *J. Am. Chem. Soc.* **1992**, *114*, 4213–4219.
- (15) Jacob, V.; Landorf, C. W.; Zakharov, L. N.; Weakley, T. J. R.; Haley, M. M. *Organometallics* **2009**, *28*, 5183–5190.
- (16) Paneque, M.; Posadas, C. M.; Poveda, M. L.; Rendón, N.; Salazar, V.; Oñate, E.; Mereiter, K. *J. Am. Chem. Soc.* **2003**, *125*, 9898–9899.

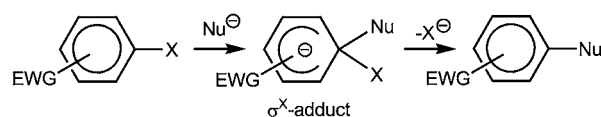
phine¹⁸ to metallabenzene ring carbon atoms and the formation of a fused ring osmabenzene through an intramolecular nucleophilic aromatic substitution reaction involving the sulfur atom of an osmabenzene thiocyanate ring substituent.¹⁹ In this paper we now extend the suite of well-defined metallabenzene reactions that have direct counterparts in classic benzene chemistry with the report of the first metallabenzene reactions that involve intermolecular nucleophilic aromatic substitution of hydrogen. Specifically, we report (i) the high yield syntheses of the cationic metallabenzenes $[\text{Ir}(\text{C}_5\text{H}_4\{\text{SMe-1}\})(\kappa^2\text{-S}_2\text{CNEt}_2)(\text{PPh}_3)_2]\text{PF}_6$ (**1**) and $[\text{Os}(\text{C}_5\text{H}_4\{\text{SMe-1}\})(\text{CO})_2(\text{PPh}_3)_2][\text{CF}_3\text{SO}_3]$ (**2**); (ii) the regioselective addition of the nucleophiles H^- , Me^- , and OEt^- to the cationic metallabenzenes **1** and **2** to give the metallacyclohexa-1,4-diene complexes $\text{Ir}(\text{C}_5\text{H}_3\{\text{SMe-1}\}\{\text{H-3}\}\{\text{Nu-3}\})(\kappa^2\text{-S}_2\text{CNEt}_2)(\text{PPh}_3)_2$ ($\text{Nu} = \text{H}$ (**3**), Me (**4**), OEt (**5**)) and $\text{Os}(\text{C}_5\text{H}_3\{\text{SMe-1}\}\{\text{H-3}\}\{\text{Nu-3}\})(\text{CO})_2(\text{PPh}_3)_2$ ($\text{Nu} = \text{H}$ (**8**), Me (**9**)); (iii) the oxidative rearomatization of the metallacyclohexa-1,4-diene rings in **3–5**, **8**, and **9** to either return the original metallabenzenes (in the case of **3** and **8**) or produce the new, substituted metallabenzenes $[\text{Ir}(\text{C}_5\text{H}_3\{\text{SMe-1}\}\{\text{Me-3}\})(\kappa^2\text{-S}_2\text{CNEt}_2)(\text{PPh}_3)_2]\text{PF}_6$ (**6**), $[\text{Ir}(\text{C}_5\text{H}_4\{\text{SMe-1}\}\{\text{OEt-3}\})(\kappa^2\text{-S}_2\text{CNEt}_2)(\text{PPh}_3)_2]\text{PF}_6$ (**7**), and $[\text{Os}(\text{C}_5\text{H}_3\{\text{SMe-1}\}\{\text{Me-3}\})(\text{CO})_2(\text{PPh}_3)_2]\text{Cl}$ (**10**) in the case of **4**, **5**, and **9**, respectively; (iv) the application of DFT calculations to rationalize the regioselectivity observed for nucleophilic attack at the metallabenzene rings of **1** and **2**; and (v) the X-ray crystal structures of **1**, **3**, **6**, and **7**.

Results and Discussion

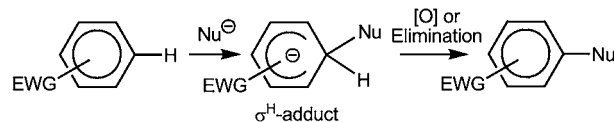
We have previously reported that the neutral metallabenzenes $\text{Os}(\text{C}_5\text{H}_4\{\text{SMe-1}\})\text{I}(\text{CO})(\text{PPh}_3)_2$ and $\text{Ir}(\text{C}_5\text{H}_4\{\text{SMe-1}\})\text{Cl}_2(\text{PPh}_3)_2$ undergo electrophilic aromatic substitution reactions that parallel the classic $\text{S}_\text{E}\text{Ar}$ reactions of benzene.^{11,12} These observations prompted us to question whether under the appropriate circumstances metallabenzenes might also participate in the complementary reaction, nucleophilic aromatic substitution of hydrogen. There are two main classes of nucleophilic aromatic substitution reactions in organic chemistry. If the nucleophile adds to a ring position that is occupied by a good leaving group X (such as halide), the intermediate σ^X -adduct undergoes rapid elimination of X^- and the corresponding substituted aromatic product is formed (see Chart 1A). This classic type of nucleophilic aromatic substitution reaction ($\text{S}_\text{N}\text{Ar}$) is well-known.²⁰ In some cases the σ^X -adduct can be isolated, and examples are provided by the Jackson–Meisenheimer complexes.²¹ If addition of the nucleophile to the arene occurs at a position occupied by hydrogen, an intermediate σ^H -adduct is formed (see Chart 1B). Since the spontaneous elimination of hydride ion from intermediates of this type rarely occurs, the conversion of these intermediates into the substituted aromatic products usually has to be achieved by alternative pathways.^{22–25} In general these involve either

Chart 1. Nucleophilic Aromatic Substitution (NAS) of the Leaving Group X or H in Benzenes and the Corresponding Reaction Involving NAS of H in Cationic Metallabenzenes

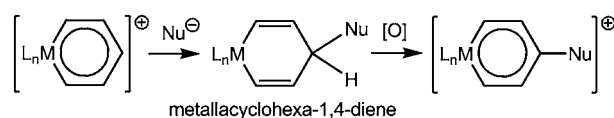
A. Classic NAS of X ($\text{S}_\text{N}\text{Ar}$)



B. NAS of hydrogen ($\text{S}_\text{N}^\text{H}$)



C. NAS of hydrogen in cationic metallabenzenes



oxidation of the σ^H -adduct or elimination of HY from this intermediate (where Y is an auxiliary group that is part of the nucleophile or a group already attached to the aromatic ring).^{22,23}

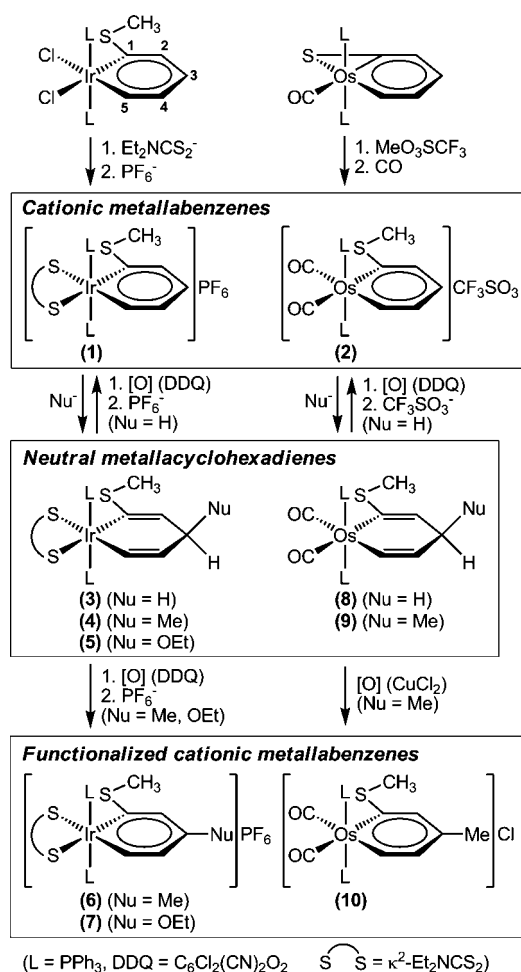
In order to investigate the nucleophilic aromatic substitution reactions of hydrogen in metallabenzenes, access to suitable substrates was required. It appeared to us that these would preferably have relatively electron-deficient metallacyclic rings, minimal ring substitution, and ancillary ligand complements that are unreactive. Since cationic metallabenzenes might exhibit reduced ring electron density²⁶ as well as favorable electrostatic interactions toward anionic nucleophiles, our attention was directed toward the synthesis of appropriate compounds of this type.

We have previously reported that the iridabenzene $\text{Ir}(\text{C}_5\text{H}_4\{\text{SMe-1}\})\text{Cl}_2(\text{PPh}_3)_2$ is readily accessible from $\text{IrCl}(\text{CS})(\text{PPh}_3)_2$.¹² The two chloride ligands in this iridabenzene are relatively labile and on treatment with $\text{NaS}_2\text{CNEt}_2$ and NEt_4PF_6 the cationic iridabenzene $[\text{Ir}(\text{C}_5\text{H}_4\{\text{SMe-1}\})(\kappa^2\text{-S}_2\text{CNEt}_2)(\text{PPh}_3)_2]\text{PF}_6$ (**1**) can be isolated directly in high yield (see Scheme 1). Characterizing data for **1** and all other new compounds are detailed in the Experimental Section. The numbering scheme used for the iridabenzene ring system is indicated in Scheme 1 and follows the numbering system normally used for metallabenzenes.² In the ^1H and ^{13}C NMR spectra of **1** the chemical shifts of the iridabenzene ring atoms appear in the regions typically observed for metallabenzenes.^{1–3} The signal for H5 is observed at a characteristically low field position (12.28 ppm), and the other metallabenzene protons display aromatic-like chemical shifts (7.09 (H4), 6.80 (H3), 5.79 (H2) ppm). Likewise, the metal-bound metallabenzene ring carbon atoms appear at typical low-field positions (235.18 (C1), 191.69 (C5) ppm) and the other ring carbon atoms are observed in the normal aromatic region (153.12 (C3), 126.77 (C4), 120.44 (C2) ppm). Somewhat unexpectedly these signals are all very close to the corresponding signals in the parent neutral iridabenzene $\text{Ir}(\text{C}_5\text{H}_4\{\text{SMe-1}\})\text{Cl}_2(\text{PPh}_3)_2$,¹² perhaps indicating that the dithiocarbamate sulfur atoms act as good electron donors toward the cationic metal center.

- (17) Paneque, M.; Posadas, C. M.; Poveda, M. L.; Rendón, N.; Santos, L. L.; Alvarez, E.; Salazar, V.; Mereiter, K.; Oñate, E. *Organometallics* **2007**, *26*, 3403–3415.
 (18) Zhang, H.; Lin, R.; Hong, G.; Wang, T.; Wen, T. B.; Xia, H. *Chem.—Eur. J.* **2010**, *16*, 6999–7007.
 (19) Wang, T.; Li, S.; Zhang, H.; Lin, R.; Han, F.; Lin, Y.; Wen, T. B.; Xia, H. *Angew. Chem., Int. Ed.* **2009**, *48*, 6453–6456.
 (20) Bunnett, J. F.; Zahler, R. E. *Chem. Rev.* **1951**, *51*, 273–412.
 (21) Terrier, F. *Chem. Rev.* **1982**, *82*, 77–152.
 (22) Makosza, M.; Wojciechowski, K. *Chem. Rev.* **2004**, *104*, 2631–2666.
 (23) Charushin, V. N.; Chupakhin, O. N. *Mendeleev Commun.* **2007**, *17*, 249–254.
 (24) van der Plas, H. *Adv. Heterocycl. Chem.* **2004**, *86*, 1–40.
 (25) Gulevskaya, A. V.; Pozharskii, A. F. *Adv. Heterocycl. Chem.* **2007**, *93*, 57–115.

- (26) Fernandez, I.; Frenking, G. *Chem.—Eur. J.* **2007**, *13*, 5873–5884.

Scheme 1. Reactions of the Cationic Metallabenzenes **1** and **2** with Nucleophiles To Form Neutral Metallacyclohexa-1,4-dienes and the Subsequent Oxidation of These To Give the Corresponding Substituted Cationic Metallabenzenes



The crystal structure of **1** has been determined, and the molecular structure of one of the two independent molecules in the unit cell (molecule A) is shown in Figure 1. The crystal and refinement data in CIF format for **1** and for the other crystal structures reported in this paper are available in the Supporting Information. The distances within the metallacyclic ring are all in accord with a metallabenzene formulation. The two Ir–C distances are equal (Ir–C1 2.009(16), Ir–C5 2.009(15) Å) and the ring C–C distances are consistent with delocalization (C1–C2 1.42(2), C2–C3 1.36(2), C3–C4 1.44(2), C4–C5 1.31(2) Å). The esd's associated with these distances are relatively large, and no significant differences can be discerned between these and the corresponding distances in the neutral precursor Ir(C₅H₄{SMe-1})Cl₂(PPh₃)₂.¹² The metallabenzene ring in **1** is not planar in the sense that the iridium atom sits 0.351 Å out of the mean plane through the five ring carbon atoms. This displacement is similar to that observed for Ir(C₅H₄{SMe-1})Cl₂(PPh₃)₂ (where this value is 0.307 Å). Similar distortions from planarity are often observed for metallabenzenes, but computational studies indicate that this does not compromise aromaticity.²⁷

The other cationic metallabenzene that was synthesized and employed in this study was [Os(C₅H₄{SMe-1})(CO)₂(PPh₃)₂]

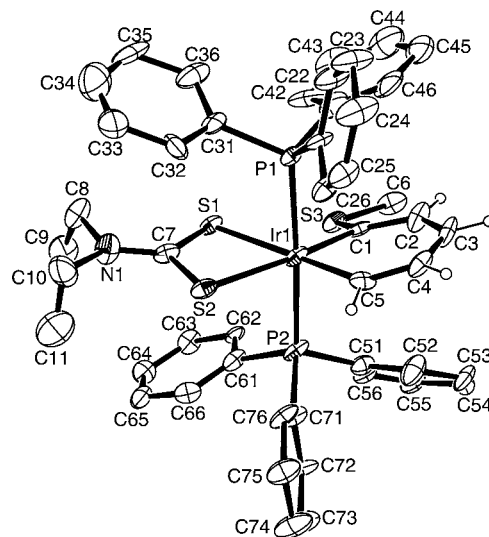


Figure 1. ORTEP diagram of the cation of **1** (molecule A) showing 30% probability displacement ellipsoids for non-hydrogen atoms and hydrogen atoms as arbitrary spheres. Hydrogen atoms on phenyl, ethyl, and methyl groups have been removed for clarity. Selected distances [Å]: Ir–C1, 2.009(16); Ir–C5, 2.009(16); C1–C2, 1.42(2); C2–C3, 1.36(2); C3–C4, 1.44(2); C4–C5, 1.31(2).

[CF₃SO₃] (**2**). Complex **2** can be conveniently obtained through sequential treatment of Os(C₅H₄{S-1})(CO)(PPh₃)₂²⁸ with CF₃SO₃CH₃ and CO. The same osmabenzene cation has been isolated previously as the perchlorate salt [Os(C₅H₄{SMe-1})(CO)₂(PPh₃)₂][ClO₄].²⁹ In the ¹H and ¹³C NMR spectra of **2** the chemical shifts of the osmabenzene ring atoms appear in the regions typically observed for other metallabenzenes.^{1–3} When compared to the ¹H and ¹³C NMR chemical shift data for the related neutral osmabenzene Os(C₅H₄{SMe-1})Cl(CO)(PPh₃)₂,³⁰ the biggest differences are found for the metallacyclic ring atoms H5 and C5 that are closely associated with the metal. Thus, in the cationic osmabenzene **2** the signals for H5 and C5 are observed at 10.82 and 199.58 ppm, respectively, whereas the signals for the corresponding atoms in Os(C₅H₄{SMe-1})Cl(CO)(PPh₃)₂ are observed at 13.27 and 220.96 ppm, respectively. The considerably higher field values observed for both H5 and C5 in **2** could indicate the π-bonding between Os and C5 is somewhat reduced upon replacement of the trans Cl ligand in Os(C₅H₄{SMe-1})Cl(CO)(PPh₃)₂ with CO.

Although the structural and NMR data obtained for **1** and **2** provided no compelling evidence that the metallabenzene carbon atoms in these cationic complexes are activated toward attack by nucleophiles, this was indeed found to be the case. Presumably the tightly coordinated and relatively unreactive ancillary ligand sets^{31,32} in these compounds successfully shield the cationic metal centers, and nucleophilic attack is diverted toward the carbon atoms of the metallabenzene rings. Thus, on treatment of an ethanol solution of **1** with NaBH₄, the green color rapidly fades and the colorless neutral iridacyclohexa-1,4-diene Ir(C₅H₃-

(28) Elliott, G. P.; McAuley, N. M.; Roper, W. R. *Inorg. Synth.* **1989**, *26*, 184–189.

(29) Elliott, G. P.; Roper, W. R.; Waters, J. M. *J. Chem. Soc., Chem. Commun.* **1982**, 811–813.

(30) Johns, P. M.; Roper, W. R.; Woodgate, S. D.; Wright, L. J. *Acta Crystallogr., Sect. E* **2009**, *E65*, m1319.

(31) Clark, A. M.; Rickard, C. E. F.; Roper, W. R.; Woodman, T. J.; Wright, L. J. *Organometallics* **2000**, *19*, 1766–1774.

(32) Clark, A. M.; Rickard, C. E. F.; Roper, W. R.; Wright, L. J. *Organometallics* **1999**, *18*, 2813–2820.

(27) Zhu, J.; Jia, G.; Lin, Z. *Organometallics* **2007**, *26*, 1986–1995.

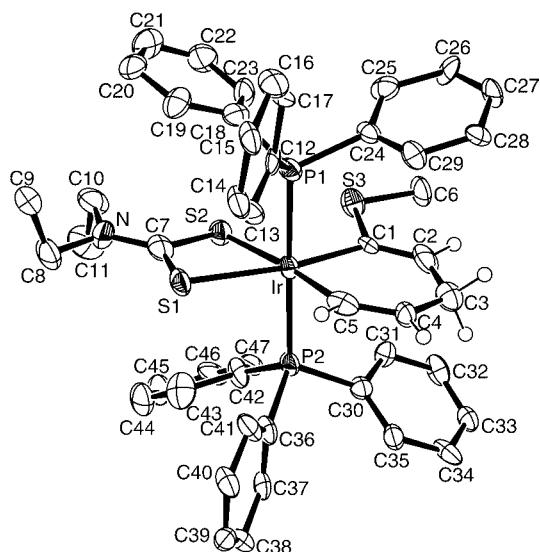


Figure 2. ORTEP diagram of **3** showing 50% probability displacement ellipsoids for non-hydrogen atoms and hydrogen atoms as arbitrary spheres. Hydrogen atoms on phenyl, ethyl, and methyl groups have been removed for clarity. Selected distances [Å]: Ir–C1, 2.046(11); Ir–C5, 2.073(12); C1–C2, 1.321(16); C2–C3, 1.460(18); C3–C4, 1.465(16); C4–C5, 1.340(16).

{SMe-1}{H₂-3})(κ²-S₂CNEt₂)(PPh₃)₂ (**3**) precipitates from solution (Scheme 1). The hydride adds selectively to C3 of **1**, saturating this atom and disrupting the π-bond delocalization within the metallacyclic ring. These changes are clearly evident in the ¹H and ¹³C NMR spectra of **3**. The two protons on the saturated C3 atom appear in the ¹H NMR spectrum as a singlet at 2.46 ppm. The resonances of the other ring protons (7.76, d, ³J_{HH} = 9.7 Hz, (H₅); 5.66, d, ³J_{HH} = 9.5 Hz, (H₄); 4.27 (s, H₂) ppm) all appear at considerably higher field positions compared with the corresponding resonances in **1** (12.28 (H₅), 7.09 (H₄), 5.79 (H₂) ppm) and are consistent with an iridacyclohexa-1,4-diene formulation. The ¹³C NMR resonances of the metallacyclic ring atoms in **3** (124.18 (C₄), 113.68 (C₂), 113.15 (C₁), 111.83 (C₅), 37.18 (C₃) ppm) also show significant shifts to higher-field values that are again consistent with two localized double bonds. Particularly noteworthy are the resonances of the metal-bound ring atoms C₁ and C₅ that have moved upfield by close to 100 ppm from the values of 235.18 and 191.69 ppm, respectively, observed in **1**.

The crystal structure of **3** has been determined, and the molecular structure is shown in Figure 2. The distances within the metallacyclic ring support an iridacyclohexa-1,4-diene formulation. The Ir–C1 (2.046(11) Å) and Ir–C5 (2.073(12) Å) distances are equal within esd limits, the C1–C2 (1.321(16) Å) and C4–C5 (1.340(16) Å) distances are consistent with double bonds, while the C2–C3 (1.460(18) Å) and C3–C4 (1.465(16) Å) separations indicate single bonds between these atoms.

Other nucleophiles also add to the iridabenzene ring of **1** at C3 to give neutral iridacyclohexa-1,4-diene products. Thus, treatment of **1** with MeLi in tetrahydrofuran gives Ir(C₅H₃{SMe-1}{H-3}{Me-3})(κ²-S₂CNEt₂)(PPh₃)₂ (**4**) (Scheme 1). The ring methyl group is observed in the ¹H NMR spectrum of **4** as a doublet at 0.57 ppm, and the chemical shifts and coupling patterns of the ring H atoms (7.57 (H₅), 5.46 (H₄), 4.44 (H₂), 2.18 (H₃) ppm) are very similar to those of **3**. The resonances of the ring carbon atoms in the ¹³C NMR spectrum of **4** (132.49 (C₄), 121.53 (C₂), 115.87 (C₁), 114.64 (C₅), 39.62 (C₃) ppm)

are also comparable to those in **3**, and together these data confirm that the methyl group is attached to C3. Unlike the situation in **3**, there is no equatorial mirror plane in **4**, and accordingly in the ³¹P NMR spectrum a four line, second order spectrum is observed for the two inequivalent, strongly coupled phosphorus atoms of the chiral complex. The inequivalent nature of the two triphenyl phosphine ligands is also evident in the two sets of resonances observed for the phenyl groups in the ¹³C NMR spectrum.

Some indication of the range of external nucleophiles that can add to **1** to give iridacyclohexa-1,4-diene products is provided by one further example, NaOEt. Treatment of **1** with this reagent results in the formation of Ir(C₅H₃{SMe-1}{H-3}{OEt-3})(κ²-S₂CNEt₂)(PPh₃)₂ (**5**) (Scheme 1). As with **3** and **4**, the ¹H NMR (7.95 (H₅); 5.70 (H₄); 4.79 (H₂); 3.41 (H₃) ppm) and ¹³C NMR (128.43 (C₄); 120.81 (C₁); 117.94 (C₅); 117.06 (C₂); 82.96 (C₃) ppm) spectral data for the ring atoms of **5** confirm that addition occurs at C3. As with **4**, the absence of an equatorial mirror plane in **5** is clearly evident from the ³¹P NMR spectrum and the resonances of the phenyl carbon atoms in the ¹³C NMR spectrum.

It is noteworthy that unlike these reactions between the cationic iridabenzene **1** and nucleophiles that form the corresponding iridacyclohexa-1,4-diene complexes, the formation of ring addition products is not observed when the parent neutral iridabenzene Ir(C₅H₄{SMe-1})Cl₂(PPh₃)₂ is treated with nucleophiles such as H⁻, Me⁻ or OEt⁻.

There is a clear relationship between the iridacyclohexa-1,4-diene complexes **3–5** and the σ^H-adducts formed as intermediates in nucleophilic aromatic substitution reactions of activated benzenes (C and B, respectively, Chart 1).^{21–24} The possibility that the metallacyclic rings in these compounds might be rearomatized through oxidation reactions that parallel those employed in the conversion of σ^H-adducts into substituted aromatic products was indicated by the observation that CDCl₃ solutions of **3** in the presence of air slowly turned green over a period of days. NMR spectroscopy showed that the green iridabenzene cation [Ir(C₅H₄{SMe-1})(κ²-S₂CNEt₂)(PPh₃)₂]⁺ was formed as the major product and after the addition of NEt₄PF₆ **1** could be isolated from solution in approximately 40% yield. In the absence of air, solutions of **3** do not undergo any appreciable change over a period of several days. Since 2,3-dichloro-5,6-dicyano-1,4-benzoquinone (DDQ) has been used extensively as an oxidant to aromatize σ^H-adducts in organic chemistry,²² the use of this reagent to rearomatize the iridacyclohexa-1,4-diene ring in **3** was investigated. It was found that on treatment of a dichloromethane solution of **3** with DDQ followed by the addition of NEt₄PF₆, **1** can be isolated from solution in approximately 70% yield (Scheme 1). Other oxidants such as ^tBuOOH and CuCl₂ also oxidize **3**, but the yields of **1** obtained from these reactions are not as high.

The closely related iridacyclohexa-1,4-dienes **4** and **5** are also rearomatized on exposure to suitable oxidants. In the case of **4**, treatment with DDQ followed by addition of NEt₄PF₆ gives the brown methyl substituted iridabenzene [Ir(C₅H₃{SMe-1}{Me-3})(κ²-S₂CNEt₂)(PPh₃)₂]⁺PF₆⁻ (**6**) in 53% yield after recrystallization (Scheme 1). The re-establishment of the iridabenzene ring is clearly indicated by the chemical shifts of the ring protons in the ¹H NMR spectrum (12.15 (H₅); 6.99 (H₄); 5.58 (H₂) ppm) and the ring carbons in the ¹³C NMR spectrum (228.78 (C₁); 189.04 (C₅); 169.66 (C₃); 131.15 (C₄); 122.58 (C₂) ppm). All these values are similar to the corresponding values observed for **1**. Upon conversion of **4** to **6** the equatorial mirror plane is

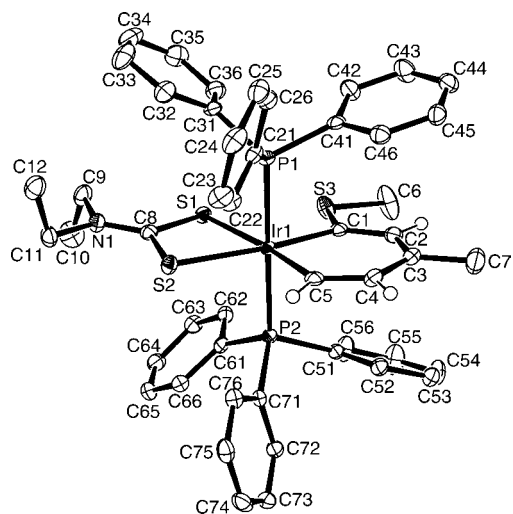


Figure 3. ORTEP diagram of the cation of **6** showing 50% probability displacement ellipsoids for non-hydrogen atoms and hydrogen atoms as arbitrary spheres. Hydrogen atoms on phenyl, ethyl, and methyl groups have been removed for clarity. Selected distances [Å]: Ir–C1, 2.011(3); Ir–C5, 2.014(3); C1–C2, 1.389(5); C2–C3, 1.382(5); C3–C4, 1.425(5); C4–C5, 1.363(4).

restored and a single resonance at -9.13 ppm is observed in the ^{31}P NMR spectrum of **6**.

The crystal structure of **6** has been determined, and the molecular structure is shown in Figure 3. The geometry about Ir is approximately octahedral with the two PPh_3 ligands mutually trans. The structure confirms that the methyl group is attached to C3 of the essentially planar iridabenzene ring. The two Ir–C distances are equal (Ir–C1, 2.011(3); Ir–C5, 2.014(3) Å), and the C–C distances within the iridabenzene ring are appropriate for a metallabenzene (C1–C2, 1.389(5); C2–C3, 1.382(5); C3–C4, 1.425(5); C4–C5, 1.363(4) Å).

The iridacyclohexadiene ring in **5** is also rearomatized on treatment with oxidizing agents. However, in this case mixtures of the ethoxy-substituted iridabenzene $[\text{Ir}(\text{C}_5\text{H}_4\{\text{SMe-1}\}\{\text{OEt-3}\})(\kappa^2\text{-S}_2\text{CNEt}_2)(\text{PPh}_3)_2]\text{PF}_6$ (**7**) and the original iridabenzene **1** are formed. The combined yield of these two metallabenzenes is relatively low when $t\text{BuOOH}$ or O_2 is the oxidant, but with DDQ equal amounts of **1** and **7** are formed in a combined yield of approximately 70%. The similarity in solubility and chromatographic behavior of these two compounds frustrated our attempts to obtain analytically pure samples of **7** that were not contaminated with small amounts of **1**. Nevertheless, we were able to obtain NMR data for **7** from samples that contained <10% of **1** as an impurity and also grow a single crystal of **7** for X-ray structure determination. The ^1H and ^{13}C NMR data for **7** confirm the iridabenzene formulation with the OEt substituent attached to C3. The resonances of the ring atoms are all similar to the corresponding values in **1** or **6** but in each case are shifted to slightly higher field values. The crystal structure of **7** has been determined, and the molecular structure is shown in Figure 4. Although the quality of the structure determination is not high, formulation as an ethoxy-substituted iridabenzene is confirmed.

Reactions between the cationic osmabenzene **2** and selected anionic nucleophiles were also investigated. Treatment of **2** with NaBH_4 in ethanol resulted in the rapid precipitation of the neutral, colorless osmacyclohexa-1,4-diene complex $\text{Os}(\text{C}_5\text{H}_3\{\text{SMe-1}\}\{\text{H}_2\text{-3}\})(\text{CO})_2(\text{PPh}_3)_2$ (**8**) (Scheme 1). The ^1H NMR chemical shifts and coupling constants of the metallacyclic ring protons are very

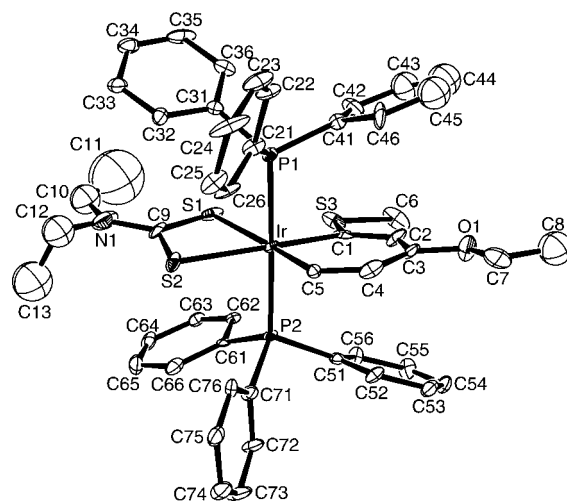


Figure 4. ORTEP diagram of the cation of **7** showing 30% probability displacement ellipsoids for non-hydrogen atoms. Selected distances [Å]: Ir–C1, 2.022(16); Ir–C5, 1.996(13); C1–C2, 1.35(2); C2–C3, 1.40(2); C3–C4, 1.447(19); C4–C5, 1.349(19).

similar to those observed for the closely related iridacyclohexa-1,4-diene **3**, and the ^{13}C NMR chemical shifts of the ring carbon atoms (132.88 (C1), 130.75 (C4), 123.35 (C5), 118.69 (C2), 38.85 (C3) ppm) are also consistent with the presence of two localized double bonds. Treatment of **2** with LiMe gave the corresponding neutral, methyl-substituted osmacyclohexa-1,4-diene complex $\text{Os}(\text{C}_5\text{H}_3\{\text{SMe-1}\}\{\text{H-3}\}\{\text{Me-3}\})(\text{CO})_2(\text{PPh}_3)_2$ (**9**) in good yield (Scheme 1). Again the metallacyclic ring resonances of **9** in the ^1H and ^{13}C NMR spectra show a striking similarity with those of the corresponding methyl-substituted iridacyclohexa-1,4-diene complex **4**, indicating that methyl addition occurs exclusively at C3. In the ^{31}P NMR spectrum of **9** a four line signal is observed for the two inequivalent, strongly coupled phosphorus atoms, as is the case for **4**. In contrast to these results, a pure ethoxy-substituted osmacyclohexa-1,4-diene analog of **5** could not be isolated from solution on treatment of **2** with NaOEt .

The neutral osmacyclohexa-1,4-diene compounds **8** and **9** are also susceptible to oxidation. In reactions that parallel those of **3–5**, treatment of **8** or **9** with oxygen, CuCl_2 , or DDQ results in rearomatization of the metallacyclic rings and formation of the corresponding cationic osmabenzenes. In the case of **8**, oxidation followed by addition of LiO_3SCF_3 gives the starting cationic osmabenzene **2**. The highest yield (ca. 80%) was obtained when DDQ was used as the oxidant. In the case of **9**, oxidation followed by the addition of LiCl yields the new cationic, methyl-substituted osmabenzene $[\text{Os}(\text{C}_5\text{H}_3\{\text{SMe-1}\}\{\text{Me-3}\})(\text{CO})_2(\text{PPh}_3)_2]\text{Cl}$ (**10**). The highest yield of **10** (ca. 50%) was obtained when CuCl_2 was used as the oxidant (Scheme 1). The resonances of the substituted osmabenzene ring atoms in the ^1H NMR spectrum (10.86 (H5), 6.97 (H4), 5.89 (H2) ppm) and ^{13}C NMR spectrum (245.91 (C1), 197.04 (C5), 171.28 (C3), 134.89 (C4), 126.15 (C2) ppm) of **10** are very similar to those observed for the parent compound **2** as well as the iridium analogue **6** and confirm the cationic osmabenzene formulation with the methyl substituent at C3. Aromatization of the metallacyclic ring in **9** restores the equatorial mirror plane, and as a result only one resonance (at 1.41 ppm) is observed for the two phosphorus atoms in the ^{31}P NMR spectrum of **10**.

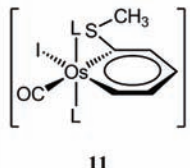
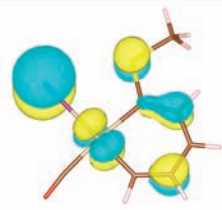
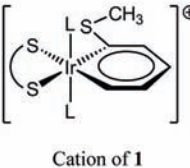
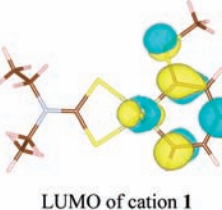
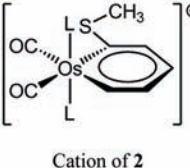
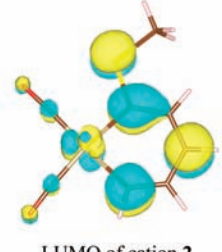
The transformations that take the metallacyclohexa-1,4-dienes **3–5**, **8**, and **9** to the corresponding cationic metallabenzenes

only occur on treatment with oxidizing agents such as O₂, DDQ, or CuCl₂. We have no data relating to the mechanisms for these oxidation reactions. Indeed, details of the mechanisms for the oxidation of simple organic σ^H -adducts with various oxidants are in most cases still not well established, and it has been proposed that the course of these reactions may vary with the oxidant.²² Electrochemical oxidation of organic σ^H -adducts to give aromatic products has been shown to proceed via stepwise transfer of two electrons and loss of H⁺, while organic σ^X -adducts are rearomatized through a one electron transfer followed by loss of X[•].³³ Further studies will be required to determine whether the oxidation reactions of the metallacyclohexa-1,4-diene complexes **3–5**, **8**, and **9** proceed by either of these mechanisms.

A report that is of direct relevance to the nucleophilic aromatic substitution reactions that produce **6**, **7**, and **10** is that on treatment of the osmabenzene Os(C₅H₃{PPh₃-2}{NCS-4})(NCS)₂(PPh₃)₂ with methoxide, the osmabenzothiazole Os(C₅H₂{PPh₃-2}{NC[OMe]S-4,5})(NCS)₂(PPh₃)₂ is formed.¹⁹ It was proposed that the mechanism of this metallabenzene ring annelation reaction involves methoxide attack at the carbon atom of a S-bound thiocyanate substituent followed by addition of the terminal nitrogen to an adjacent carbon of the metallabenzene ring to form a fused-ring osmacyclohexa-1,3-diene intermediate. Subsequent loss of hydrogen anion from the saturated ring carbon of this undetected intermediate gives the aromatic osmabenzothiazole product and H₂ after combination of the hydrogen anion with solvent. The overall process can be described as an intramolecular nucleophilic aromatic substitution of hydrogen. The proposed osmacyclohexadiene intermediate is related to the isolated complexes **3–5**, **8**, and **9** reported here, although it should be noted that hydride ion is not spontaneously lost from these complexes and rearomatization only occurs upon treatment with an oxidizing agent. A few other examples that involve the conversion of isolated metallacyclohexadienes to metallabenzenes have been reported,^{16,34} but none are part of a sequence involving nucleophilic aromatic substitution of hydrogen.

The susceptibility of the metallabenzene ring carbon atoms in **1** and **2** toward nucleophilic attack and the high regioselectivity of these reactions (only products where addition has occurred at C3 have been detected) prompted us to investigate whether these observations could be rationalized by computational studies. The condensed Fukui function derived from DFT can be used to predict the most nucleophilic site (the atom with largest f_k^- value) and the most electrophilic site (the atom with largest f_k^+ value) of a molecule.³⁵ Although there has been some discussion of the shortcomings of this method,³⁶ it has been successfully employed as a reactivity index that does, for example, correctly predict the observed electrophilic substitution patterns for a range of aromatic heterocyclic compounds.³⁷ Therefore it appeared that this method might also be suitable for investigating the reactivity of the metallabenzenes such as **1** and **2**. To test this possibility the condensed Fukui function was initially computed for the osmabenzene Os(C₅H₄{SMe-

Table 1. Condensed Fukui Functions (FF) for (**11**) (f_k^-), the Cation of **1** (f_k^+), and the Cation of **2** (f_k^+) (L = PPh₃)^a

Compound	Atom	FF	MO picture
 11	C1	0.00	 HOMO of 11
	C2	0.09	
	C3	-0.01	
	C4	0.11	
	C5	0.00	
 Cation of 1	C1	0.15	 LUMO of cation 1
	C2	-0.02	
	C3	0.18	
	C4	-0.03	
	C5	0.16	
 Cation of 2	C1	0.15	 LUMO of cation 2
	C2	-0.03	
	C3	0.17	
	C4	-0.03	
	C5	0.17	

^a Molecular orbital pictures (at isosurface level 0.04) for **11** (HOMO), **1** (LUMO), and **2** (LUMO) with PPh₃ ligands removed for clarity of viewing.

})I(CO)(PPh₃)₂ (**11**) which has been reported to undergo electrophilic aromatic substitution exclusively at C4 (the ring position *para* to the SMe group).¹¹ The results of these calculations are presented in Table 1. The ring atom C4 in **11** clearly has the largest computed f_k^- value, and this is fully in accord with the observations that electrophiles preferentially attack this atom. The fully optimized structure of the complete molecule was used in this and all the other calculations described below because in a preliminary study we found that if PH₃ is used as a model for the PPh₃ ligands the results obtained are less reliable. Details of these and all other calculations are presented in the Experimental Section.

In view of the successful application of the condensed Fukui function in this particular case, we then computed the condensed Fukui functions for the metallabenzenes **1** and **2** to determine whether this same approach could be used to explain the observation that nucleophiles preferentially attack C3 in these molecules. The computed f_k^+ values for the metallabenzene ring atoms of **1** and **2** are collected in Table 1. In the case of **1**, C1, C3, and C5 all have relatively large f_k^+ values indicating that nucleophilic attack at each of these atoms is electronically favorable. Although the differences between the f_k^+ values for these atoms are very small, the largest numerical value of f_k^+ is found for C3 which is consistent with the observation that this is the preferred site for nucleophilic attack. As might be expected, visual inspection of the LUMO shows that the most significant lobes are also localized at C1, C3, and C5 (see Table

(33) Gallardo, I.; Guirado, G.; Marquet, J. *J. Org. Chem.* **2002**, *67*, 2548–2555.

(34) Bleeke, J. R.; Xie, Y. F.; Peng, W. J.; Chiang, M. *J. Am. Chem. Soc.* **1989**, *111*, 4118–4120.

(35) Parr, R. G.; Yang, W. *Density-Functional Theory of Atoms and Molecules*; Oxford University Press: New York, USA, 1989.

(36) Otero, N.; Mandado, M.; Mosquera, R. A. *J. Chem. Phys.* **2007**, *126*, 2341081–6.

(37) Martínez, A.; Vázquez, M.-V.; Carreón-Macedo, J. L.; Sansores, L. E.; Salcedo, R. *Tetrahedron* **2003**, *59*, 6415–6422.

1). A similar situation is observed for **2**. Again C1, C3, and C5 all have the largest f_k^+ values, and the significant lobes of the LUMO are again localized at C1, C3, and C5. In this case the f_k^+ values for C3 and C5 are the same, indicating that electronically these are equally favorable sites for nucleophilic attack. However, the observed clear preference for attack at C3 in this compound, as well as in **1**, demonstrates that application of the condensed Fukui function alone to this class of compounds does have limitations. It is noteworthy that this computational method does not take into consideration steric effects, and in the reactions of **1** and **2** with nucleophiles steric congestion could be an important factor that results in discrimination between sites with similarly favorable f_k^+ values. Inspection of the structures of **1** and **2** clearly indicates that, of the atoms C1, C3, and C5, it is C3 that is the most accessible to external reagents, and this may explain the observed preference for nucleophilic attack to occur here.

Concluding Remarks

The addition of appropriate nucleophiles to the cationic metallabenzene **1** and **2** to give the isolated metallacyclohexa-1,4-dienes **4**, **5**, and **9** and the subsequent oxidation of these compounds to yield the corresponding substituted cationic metallabenzene **6**, **7**, and **10**, respectively, provide the first examples in metallabenzene chemistry of regioselective nucleophilic aromatic substitution of hydrogen by external nucleophiles. The direct correspondence of these transformations to the classic nucleophilic aromatic substitution of hydrogen in simple benzenes is illustrated by the sequences B and C in Chart 1. The observation that both the iridabenzene **1** and the osmabenzene **2** participate in nucleophilic aromatic substitution reactions indicates that this reaction class for metallabenzenes could evolve into one of considerable scope. The high regioselectivity observed for these reactions can be rationalized by consideration of the condensed Fukui functions for **1** and **2**. While this method successfully predicts the electronically preferred sites for nucleophilic attack, steric factors also clearly play a role in determining the outcome of these reactions.

Experimental Section

Standard laboratory procedures were followed as have been described previously.³⁸ Infrared spectra (4000–400 cm^{-1}) of solid samples were recorded on a Perkin-Elmer Spectrum 400 spectrometer using an ATR accessory. NMR spectra were obtained on a Bruker Avance 300 at 25 °C. ^1H , ^{13}C , ^{31}P , and ^{19}F NMR spectra were obtained operating at 300.13 (^1H), 75.48 (^{13}C), 121.50 (^{31}P), and 282.4 (^{19}F) MHz, respectively. Resonances are quoted in ppm, and ^1H NMR spectra were referenced to either tetramethylsilane (0.00 ppm) or the proteo-impurity in the solvent (7.25 ppm for CHCl_3). ^{13}C NMR spectra were referenced to CDCl_3 (77.00 ppm), ^{31}P NMR spectra to 85% orthophosphoric acid (0.00 ppm) as an external standard, and ^{19}F NMR spectra to CFCl_3 (0.00 ppm) as an external standard. High resolution mass spectra were recorded using the fast atom bombardment technique with a Varian VG 70-SE mass spectrometer or electrospray ionization using a Bruker Daltronics MicroTOF instrument. Elemental analyses were obtained from the Microanalytical Laboratory, University of Otago.

Synthesis of $[\text{Ir}(\text{C}_5\text{H}_4\{\text{SMe-1}\})(\kappa^2\text{-S}_2\text{CNET}_2)(\text{PPh}_3)_2]\text{PF}_6$ (1**).** $\text{Ir}(\text{C}_5\text{H}_4\{\text{SMe-1}\})\text{Cl}_2(\text{PPh}_3)_2$ ¹² (50 mg, 0.056 mmol) and sodium diethyldithiocarbamate (15 mg, 0.067 mmol) were added to a degassed frozen mixture of dichloromethane (9 mL) and ethanol (2 mL). The Schlenk tube was evacuated, sealed, warmed to room

temperature and allowed to stir for 15 min. During this time the purple solution gradually turned green. The solvent was then removed under reduced pressure, and the resultant solid recrystallized from dichloromethane/ethanol in the presence of NEt_4PF_6 to give pure **1** as emerald green crystals (52 mg, 82%). The crystal for X-ray structure determination was grown from 1,2-dichloroethane/ethanol. Anal. Calcd for $\text{C}_{47}\text{H}_{47}\text{F}_6\text{IrNP}_6\text{S}_3 \cdot 0.5(\text{CH}_2\text{Cl}_2)$: C, 49.03; H, 4.16; N, 1.20. Found: C, 49.19; H, 4.45; N, 1.42% (^1H NMR spectrum shows presence of ca. 0.5 mol equiv of CH_2Cl_2 in the analytical sample). MS (m/z , FAB+, NBA): calcd for $\text{C}_{47}\text{H}_{47}^{193}\text{IrNP}_6\text{S}_3 [\text{M} - \text{PF}_6]^+$, 976.1975; found, 976.1991. ^1H NMR (CDCl_3 , δ): 12.28 (d, $^3J_{\text{HH}} = 9.2$ Hz, H5); 7.41–7.26 (m, 30H, PPh₃); 7.09 (apparent t, $^3J_{\text{HH}} = 8.0$ Hz, 1H, H4); 6.80 (apparent t, $^3J_{\text{HH}} = 9.0$ Hz, 1H, H3); 5.79 (d, $^3J_{\text{HH}} = 9.2$ Hz, 1H, H2); 3.03 (q, $^3J_{\text{HH}} = 6.9$ Hz, 2H, $\text{S}_2\text{CN}(\text{CH}_2\text{CH}_3)_2$); 2.69 (q, $^3J_{\text{HH}} = 6.9$ Hz, 2H, $\text{S}_2\text{CN}(\text{CH}_2\text{CH}_3)_2$); 2.12 (s, 3H, SCH_3); 0.84 (t, $^3J_{\text{HH}} = 7.2$ Hz, 3H, $\text{S}_2\text{CN}(\text{CH}_2\text{CH}_3)_2$); 0.58 (t, $^3J_{\text{HH}} = 7.2$ Hz, 3H, $\text{S}_2\text{CN}(\text{CH}_2\text{CH}_3)_2$). ^{13}C NMR (CDCl_3 , δ): 235.18 (t, $^2J_{\text{CP}} = 4.7$ Hz, C1); 204.40 (s, $\text{S}_2\text{CN}(\text{CH}_2\text{CH}_3)_2$); 191.69 (t, $^2J_{\text{CP}} = 8.5$ Hz, C5); 153.12 (s, C3); 134.82 (t, $^3,^5J_{\text{CP}} = 9.3$ Hz, *m*-PPh₃); 130.80 (s, *p*-PPh₃); 128.11 (t, $^1,^3J_{\text{CP}} = 56.4$ Hz, *i*-PPh₃); 127.54 (t, $^2,^4J_{\text{CP}} = 9.9$ Hz, *o*-PPh₃); 126.77 (s, C4); 120.44 (s, C2); 44.85 (s, $\text{S}_2\text{CN}(\text{CH}_2\text{CH}_3)_2$); 44.06 (s, $\text{S}_2\text{CN}(\text{CH}_2\text{CH}_3)_2$); 22.56 (s, SCH_3); 12.20 (s, $\text{S}_2\text{CN}(\text{CH}_2\text{CH}_3)_2$); 11.71 (s, $\text{S}_2\text{CN}(\text{CH}_2\text{CH}_3)_2$). ^{31}P NMR (CDCl_3 , δ): -9.44 (s). ^{19}F NMR (CDCl_3 , δ): -144.3 (septuplet, $^1J_{\text{PF}} = 712.5$ Hz, PF_6).

Synthesis of $[\text{Os}(\text{C}_5\text{H}_4\{\text{SMe-1}\})(\text{CO})_2(\text{PPh}_3)_2][\text{CF}_3\text{SO}_3]$ (2**).** $\text{Os}(\text{C}_5\text{H}_4\{\text{S-1}\})(\text{CO})(\text{PPh}_3)_2$ (500 mg, 0.596 mmol) was dissolved in toluene (10 mL), and methyl trifluoromethanesulfonate (135 μL , 1.19 mmol) was added. The brown solution was left to stir for 1 h during which time a purple suspension formed. The purple solid was collected by filtration and then was resuspended in toluene (10 mL) in a Fischer–Porter flask and placed under CO (20 psi) for 24 h. The purple suspension changed to a red suspension during this time. The product was collected by filtration and washed with hexane to give pure **2** as a red solid (553 mg, 90%). Anal. Calcd for $\text{C}_{45}\text{H}_{37}\text{F}_3\text{O}_2\text{OsP}_2\text{S}_2 \cdot \text{H}_2\text{O}$: C, 51.52; H, 3.75. Found: C, 51.58; H, 3.73% (^1H NMR spectrum shows presence of ca. 1 mol equiv of H_2O in the analytical sample). MS (m/z , FAB+, NBA): calcd for $\text{C}_{44}\text{H}_{37}\text{O}_2^{192}\text{OsP}_2\text{S} [\text{M} - \text{CF}_3\text{SO}_3]^+$, 883.1604; found, 883.1578. IR (cm^{-1}): 2034(s) $\nu(\text{CO})$, 1973(s) $\nu(\text{CO})$, 1264(s), 1157(s), 1030(s) $\nu(\text{CF}_3\text{SO}_3)$. ^1H NMR (CDCl_3 , δ): 10.82 (d, $^3J_{\text{HH}} = 11.1$ Hz, H5); 7.49–7.27 (m, 30H, PPh₃); 7.08 (apparent t, $^3J_{\text{HH}} = 8.3$ Hz, 1H, H3); 7.01 (apparent t, $^3J_{\text{HH}} = 8.3$ Hz, 1H, H4); 6.42 (d, $^3J_{\text{HH}} = 9.4$ Hz, 1H, H2); 2.16 (s, 3H, SCH_3). ^{13}C NMR (CDCl_3 , δ): 250.97 (t, $^2J_{\text{CP}} = 6.5$ Hz, C1); 199.58 (t, $^2J_{\text{CP}} = 10.1$ Hz, C5); 181.76 (t, $^2J_{\text{CP}} = 9.4$ Hz, CO); 179.63, $^2J_{\text{CP}} = 7.8$ Hz, CO); 154.32 (s, C3); 133.43 (t, $^3,^5J_{\text{CP}} = 10.7$ Hz, *m*-PPh₃); 131.59 (s, *p*-PPh₃); 130.09 (s, C4); 129.79 (t, $^1,^3J_{\text{CP}} = 56.4$ Hz, *i*-PPh₃); 128.62 (t, $^2,^4J_{\text{CP}} = 10.6$ Hz, *o*-PPh₃); 124.20 (s, C2); 24.88 (s, SCH_3). ^{31}P NMR (CDCl_3 , δ) 1.99 (s).

Synthesis of $[\text{Ir}(\text{C}_5\text{H}_3\{\text{SMe-1}\})(\text{H}_2\text{-3})(\kappa^2\text{-S}_2\text{CNET}_2)(\text{PPh}_3)_2]$ (3**).** **1** (50 mg, 0.045 mmol) was added to ethanol (8 mL). NaBH_4 (22 mg, 0.58 mmol) was dissolved in ethanol (3 mL), and the solution was filtered through Celite. The NaBH_4 /ethanol solution was added slowly to the solution of **1** in ethanol until the green color faded and a white precipitate formed. The suspension was stirred for 10 min, and the solid was collected by filtration and then recrystallized from dichloromethane/ethanol to give pure **3** as silvery-white fine crystals (30 mg, 68%). The crystal for X-ray structure determination was grown from 1,2-dichloroethane/ethanol. Anal. Calcd for $\text{C}_{47}\text{H}_{48}\text{IrNP}_6\text{S}_3$: C, 57.76; H, 4.95; N, 1.43. Found: C, 57.93; H, 4.80; N, 1.42%. MS (m/z , FAB+, NBA): calcd for $\text{C}_{47}\text{H}_{47}^{193}\text{IrNP}_6\text{S}_3 [\text{M} - \text{H}]^+$, 976.1975; found, 976.1973. ^1H NMR (CDCl_3 , δ): 7.76 (bd, $^3J_{\text{HH}} = 9.7$ Hz, 1H, H5); 7.65–7.61, 7.29–7.16 (m, 30H, PPh₃); 5.66 (bd, $^3J_{\text{HH}} = 9.5$ Hz, 1H, H4); 4.27 (bs, 1H, H2); 3.07 (q, $^3J_{\text{HH}} = 7.0$ Hz, 2H, $\text{S}_2\text{CN}(\text{CH}_2\text{CH}_3)_2$); 2.68 (q, $^3J_{\text{HH}} = 7.0$ Hz, 2H, $\text{S}_2\text{CN}(\text{CH}_2\text{CH}_3)_2$); 2.46 (bs, 2H, H3); 1.53 (s, 3H, SCH_3); 0.82 (t, $^3J_{\text{HH}} = 7.0$ Hz, $\text{S}_2\text{CN}(\text{CH}_2\text{CH}_3)_2$); 0.56 (t, $^3J_{\text{HH}} = 7.0$ Hz, $\text{S}_2\text{CN}(\text{CH}_2\text{CH}_3)_2$). ^{13}C NMR (CDCl_3 , δ): 208.00 (s, $\text{S}_2\text{CNCH}_2\text{CH}_3$);

(38) Maddock, S. M.; Rickard, C. E. F.; Roper, W. R.; Wright, L. J. *Organometallics* **1996**, *15*, 1793–1803.

135.48 (t, $^3J_{CP} = 9.3$ Hz, *m*-PPh₃); 131.96 (t', $^1J_{CP} = 51.3$ Hz, *i*-PPh₃); 128.68 (s, *p*-PPh₃); 126.35 (t', $^2J_{CP} = 9.2$ Hz, *o*-PPh₃); 124.18 (t, $^3J_{CP} = 3.9$ Hz, *C4*); 113.68 (s, *C2*); 113.15 (t, $^2J_{CP} = 8.90$ Hz, *C1*); 111.83 (t, $^2J_{CP} = 11.1$ Hz, *C5*); 43.52 (s, S₂CNCH₂CH₃); 42.86 (s, S₂CNCH₂CH₃); 37.18 (s, *C3*); 18.39 (s, SCH₃); 12.48 (s, S₂CNCH₂CH₃); 11.88 (s, S₂CNCH₂CH₃). ^{31}P NMR (CDCl₃, δ): -4.62 (s).

Synthesis of Ir(C₅H₃{SMe-1}{H-3})(κ²-S₂CNEt₂)(PPh₃)₂ (4). **1** (100 mg, 0.0892 mmol) was dissolved in THF (10 mL), and MeLi (111 μL of a 1.6 M solution in Et₂O, 0.178 mmol) was slowly added with stirring. The green color rapidly faded to light brown, and after a few minutes the solvent was removed under reduced pressure. The resulting brown product was purified by recrystallization from dichloromethane/ethanol to give pure **4** as colorless crystals (45 mg 51%). Anal. Calcd for C₄₈H₅₀IrNP₂S₃: C, 58.16; H, 5.08; N, 1.41. Found: C, 58.47; H, 5.06; N, 1.70%. MS (*m/z*, ES⁺): calcd for C₄₈H₄₉¹⁹³IrNP₂S₃ [M - H]⁺, 990.2126; found, 990.2175. ^1H NMR (CDCl₃, δ): 7.80–7.15 (m, 30H, PPh₃); 7.57 (obscured by PPh₃ signals, position estimated from COSY spectrum), *H5*); 5.46 (dm, $^3J_{HH} = 9.6$ Hz, 1H, *H4*); 4.44 (bs, 1H, *H2*); 3.07 (m, 1H, S₂CN(CH₂CH₃)₂); 2.90 (m, 1H, S₂CN(CH₂CH₃)₂); 2.74 (m, 1H, S₂CN(CH₂CH₃)₂); 2.57 (m, 1H, S₂CN(CH₂CH₃)₂); 2.18 (m, 1H, *H3*); 1.62 (s, 3H, SCH₃); 0.81 (m, 3H, S₂CN(CH₂CH₃)₂); 0.57 (d, $^3J_{HH} = 9.6$ Hz, 3H, CH₃); 0.56 (m, 3H, S₂CN(CH₂CH₃)₂). ^{13}C NMR (CDCl₃, δ): 208.69 (s, S₂CN(CH₂CH₃)₂); 135.66 (m, *m*-PPh₃); 132.72 (dd, $^1J_{CP} = 37.7$ Hz, $^3J_{CP} = 14.3$ Hz, *i*-PPh₃); 132.49 (apparent t, $^3J_{CP} = 4.5$ Hz, *C4*); 130.87 (dd, $^1J_{CP} = 37.4$ Hz, $^3J_{CP} = 14.3$ Hz, *i*-PPh₃); 128.78 (m, *p*-PPh₃); 128.72 (m, *p*-PPh₃); 126.35 (m, *o*-PPh₃); 121.53 (apparent t, $^3J_{CP} = 3.0$ Hz, *C2*); 115.87 (apparent t, $^2J_{CP} = 8.1$ Hz, *C1*); 114.64 (apparent t, $^2J_{CP} = 10.6$ Hz, *C5*); 43.75 (s, S₂CN(CH₂CH₃)₂); 43.23 (s, S₂CN(CH₂CH₃)₂); 39.62 (s, *C3*); 22.58 (s, CH₃); 18.41 (s, SCH₃); 12.63 (s, S₂CN(CH₂CH₃)₂); 11.98 (s, S₂CN(CH₂CH₃)₂). ^{31}P NMR (CDCl₃, δ): -3.07(*wk*), -6.75(*st*), -7.35(*st*), -11.03(*wk*).

Synthesis of Ir(C₅H₃{SMe-1}{H-3})(κ²-S₂CNEt₂)(PPh₃)₂ (5). **1** (50 mg, 0.045 mmol) was dissolved in ethanol (10 mL), and a solution of NaOEt in ethanol (50 mL, 0.97 M, 0.49 mmol) was slowly added. During the addition the green color dissipated and an off-white suspension formed. This was collected by vacuum filtration and recrystallized from dichloromethane/ethanol to give pure **5** as fine, off-white crystals (33 mg, 73%). Anal. Calcd for C₄₉H₅₂IrNOP₂S₃·CH₂Cl₂: C, 54.29; H, 4.92; N, 1.27. Found: C, 54.48; H, 4.83; N, 1.36% (^1H NMR spectrum shows presence of ca. 1 mol equiv of CH₂Cl₂ in the analytical sample). MS (*m/z*, FAB⁺, NBA): calcd for C₄₉H₅₁¹⁹³IrNOP₂S₃ [M - H]⁺, 1020.2237; found 1020.2246. ^1H NMR (CDCl₃, δ): 7.95 (bd, $^3J_{HH} = 9.6$ Hz, 1H, *H5*); 7.65–7.59, 7.29–6.90 (m, 30H, PPh₃); 5.70 (bd, $^3J_{HH} = 9.9$ Hz, 1H, *H4*); 4.79 (s, 1H, *H2*); 3.41 (m, 1H, *H3*); 3.25 (m, 1H, OCH₂CH₃); 3.07 (m, 2H, OCH₂CH₃ and S₂CN(CH₂CH₃)₂); 2.91 (m, 1H, S₂CN(CH₂CH₃)₂); 2.82 (m, 1H, S₂CN(CH₂CH₃)₂); 2.48 (m, 1H, S₂CN(CH₂CH₃)₂); 1.56 (s, 3H, SCH₃); 1.03 (apparent t, $^3J_{HH} = 6.9$ Hz, 3H, OCH₂CH₃); 0.81 (apparent t, $^3J_{HH} = 7.2$ Hz, 3H, S₂CN(CH₂CH₃)₂); 0.55 (apparent t, $^3J_{HH} = 7.2$ Hz, 3H, S₂CN(CH₂CH₃)₂). ^{13}C NMR (CDCl₃, δ): 208.14 (s, S₂CN(CH₂CH₃)₂); 135.80 (dd, $^3J_{CP} = 6.7$ Hz, $^5J_{CP} = 2.4$ Hz, *m*-PPh₃); 135.43 (dd, $^3J_{CP} = 6.7$ Hz, $^5J_{CP} = 2.3$ Hz, *m*-PPh₃); 132.33 (dd, $^1J_{CP} = 39.5$ Hz, $^3J_{CP} = 11.8$ Hz, *i*-PPh₃); 129.97 (dd, $^1J_{CP} = 40.3$ Hz, $^3J_{CP} = 11.8$ Hz, *i*-PPh₃); 128.88 (bs, *p*-PPh₃); 128.43 (s, *C4*); 126.56 (dd, $^2J_{CP} = 7.9$ Hz, $^4J_{CP} = 1.6$ Hz, *o*-PPh₃); 126.37 (dd, $^2J_{CP} = 7.8$ Hz, $^4J_{CP} = 1.6$ Hz, *o*-PPh₃); 120.81 (apparent t, $^2J_{CP} = 8.0$ Hz, *C1*); 117.94 (apparent t, $^2J_{CP} = 10.4$ Hz, *C5*); 117.06 (bs, *C2*); 82.96 (s, *C3*); 62.84 (s, OCH₂CH₃); 43.73 (s, S₂CN(CH₂CH₃)₂); 43.15 (s, S₂CN(CH₂CH₃)₂); 18.37 (s, SCH₃); 15.95 (s, OCH₂CH₃); 12.57 (s, S₂CN(CH₂CH₃)₂); 11.94 (s, S₂CN(CH₂CH₃)₂). ^{31}P NMR (CDCl₃, δ): -2.58(*wk*), -6.15(*st*), -7.08(*st*), -10.65(*wk*).

Synthesis of [Ir(C₅H₃{SMe-1}{Me-3})(κ²-S₂CNEt₂)(PPh₃)₂]PF₆ (6). **4** (100 mg, 0.101 mmol) was dissolved in dichloromethane (10 mL) contained in a Schlenk tube, and the solution was frozen. 2,3-Dichloro-5,6-dicyano-1,4-benzoquinone (DDQ) (27 mg, 0.12 mmol)

was added under nitrogen, and the tube was evacuated. The solution was allowed to warm to room temperature under vacuum, and the solution turned dark brown as this occurred. Isopropanol was added, and the dichloromethane was removed under reduced pressure to give a brown solid. Recrystallization of this material from dichloromethane/isopropanol gave pure **6** as dark brown colored crystals (49 mg, 43%). The crystal for X-ray structure determination was grown from 1,2-dichloroethane/ethanol. Anal. Calcd for C₄₈H₄₉F₆IrNP₃S₃: C, 50.78; H, 4.35; N, 1.23. Found: C, 50.57; H, 4.39; N, 1.12%. MS (*m/z*, ES⁺): calcd for C₄₈H₄₉¹⁹³IrNP₂S₃ [M - PF₆]⁺, 990.2126; found, 990.2091. ^1H NMR (CDCl₃, δ): 12.15 (dt, $^3J_{HH} = 9.0$ Hz, $^3J_{HP} = 2.0$ Hz, *H5*); 7.42–7.29 (m, 30H, PPh₃); 6.99 (d, $^3J_{HH} = 9.2$ Hz, 1H, *H4*); 5.58 (s, 1H, *H2*); 3.05 (q, $^3J_{HH} = 7.2$ Hz, 2H, S₂CN(CH₂CH₃)₂); 2.68 (q, $^3J_{HH} = 7.2$ Hz, 2H, S₂CN(CH₂CH₃)₂); 2.08 (s, 3H, SCH₃); 1.67 (s, 3H, CH₃); 0.85 (t, $^3J_{HH} = 7.1$ Hz, 3H, S₂CN(CH₂CH₃)₂); 0.57 (t, $^3J_{HH} = 7.2$ Hz, 3H, S₂CN(CH₂CH₃)₂). ^{13}C NMR (CDCl₃, δ): 228.78 (t, $^2J_{CP} = 4.5$ Hz, *C1*); 204.34 (s, S₂CN(CH₂CH₃)₂); 189.04 (t, $^2J_{CP} = 8.7$ Hz, *C5*); 169.66 (s, *C3*); 134.66 (t', $^3J_{CP} = 9.1$ Hz, *m*-PPh₃); 131.15 (s, *C4*); 130.74 (s, *p*-PPh₃); 128.32 (t', $^1J_{CP} = 56.6$ Hz, *i*-PPh₃); 127.50 (t', $^2J_{CP} = 9.8$ Hz, *o*-PPh₃); 122.58 (s, *C2*); 44.79 (s, S₂CN(CH₂CH₃)₂); 43.97 (s, S₂CN(CH₂CH₃)₂); 26.50 (s, CH₃); 22.00 (s, SCH₃); 12.16 (s, S₂CN(CH₂CH₃)₂); 11.66 (s, S₂CN(CH₂CH₃)₂). ^{31}P NMR (CDCl₃, δ): -9.13 (s).

Synthesis of [Ir(C₅H₄{SMe-1}{OEt-3})(κ²-S₂CNEt₂)(PPh₃)₂]PF₆ (7). **5** (50 mg, 0.049 mmol) and DDQ (12.2 mg, 0.0541 mmol) were added to a Schlenk tube containing frozen degassed dichloromethane (8 mL). The Schlenk tube was evacuated, sealed, allowed to warm to room temperature, and then stirred for 5 min. The pale yellow solution gradually turned deep reddish brown during this time. The solvent was then removed under reduced pressure, and the resulting brown residue was dissolved in a minimal amount of dichloromethane/ethanol (98:2) solution and purified by column chromatography (alumina) eluting with dichloromethane/ethanol (98:2). The green-yellow band was collected and crystallized from dichloromethane/ethanol in the presence of NEt₄PF₆ to produce a green-yellow solid. Analysis of this product by ^1H and ^{31}P NMR spectroscopy showed it to be **7** contaminated with **1** (20–40%). This impure product could be further purified by column chromatography on Sephadex LH-20 using methanol/dichloromethane (90:10) as eluent. Samples of **7** contaminated with about 10% **1** could be obtained in this way (ca. 20 mg obtained). The presence of **1** as a contaminant in samples of **7** precluded satisfactory elemental analysis being obtained for **7**. However **7** has been characterized by high resolution MS, NMR spectroscopy (after subtraction of signals due to **1**), and X-ray crystal structure determination (the crystal was grown from dichloromethane/hexane). MS (*m/z*, FAB⁺, NBA): calcd for C₄₉H₅₁¹⁹³IrNOP₂S₃ [M - PF₆]⁺, 1020.2237; found, 1020.2246. ^1H NMR (CDCl₃, δ): 11.60 (d, $^3J_{HH} = 10.7$ Hz, 1H, *H5*); 7.48–7.26 (m, 30H, PPh₃); 6.83 (d, $^3J_{HH} = 10.7$ Hz, 1H, *H4*); 5.28 (s, 1H, *H2*); 3.66 (q, $^3J_{HH} = 7.3$ Hz, 2H, OCH₂CH₃); 3.05 (q, $^3J_{HH} = 7.3$ Hz, 2H, S₂CN(CH₂CH₃)₂); 2.66 (q, $^3J_{HH} = 7.3$ Hz, 2H, S₂CN(CH₂CH₃)₂); 2.07 (s, 3H, SCH₃); 1.27 (t, $^3J_{HH} = 7.3$ Hz, 3H, OCH₂CH₃); 0.84 (t, $^3J_{HH} = 7.3$ Hz, 3H, S₂CN(CH₂CH₃)₂); 0.55 (t, $^3J_{HH} = 7.3$ Hz, 3H, S₂CN(CH₂CH₃)₂). ^{13}C NMR (CDCl₃, δ): 215.20 (s, *C1*); 204.41 (s, S₂CN(CH₂CH₃)₂); 178.15 (s, *C5*); 141.27 (s, *C3*); 134.73 (t', $^3J_{CP} = 9.4$ Hz, *m*-PPh₃); 130.64 (s, *p*-PPh₃); 128.71 (t', $^1J_{CP} = 55.6$, *i*-PPh₃); 127.35 (t', $^2J_{CP} = 9.4$, *o*-PPh₃); 124.14 (s, *C4*); 107.33 (s, *C2*); 65.70 (s, OCH₂CH₃); 44.53 (s, S₂CN(CH₂CH₃)₂); 43.67 (s, S₂CN(CH₂CH₃)₂); 22.48 (s, SCH₃); 14.13 (s, OCH₂CH₃); 12.17 (s, S₂CNCH₂CH₃); 11.65 (s, S₂CNCH₂CH₃). ^{31}P NMR (CDCl₃, δ): -9.63 (s).

Synthesis of Os(C₅H₃{SMe-1}{H₂-3})(CO)₂(PPh₃)₂ (8). **2** (200 mg, 0.194 mmol) was dissolved in ethanol (10 mL). NaBH₄ (22 mg, 0.58 mmol) was dissolved in ethanol (3 mL), and the solution was filtered through Celite. The NaBH₄/ethanol solution was added slowly to the solution of **2** until the red color faded (ca. 1 mL), and a white precipitate formed. The white precipitate was collected by filtration, washed with ethanol/hexane, and recrystallized from

Table 2. X-ray Structure Summary Table for **1**, **3**, **6**, and **7**

	1	3	6 ·C ₂ H ₄ Cl ₂	7
Formula	C ₄₇ H ₄₇ IrNP ₂ S ₃ ·PF ₆	C ₄₇ H ₄₄ IrNP ₂ S ₃	C ₄₈ H ₄₉ IrNP ₂ S ₃ ·PF ₆ ·C ₂ H ₄ Cl ₂	C ₄₉ H ₅₁ IrNOP ₂ S ₃ ·PF ₆
Molecular weight	1121.15	973.15	1234.12	1165.2
Crystal system	Triclinic	Monoclinic	Monoclinic	Triclinic
Space group	<i>P</i> $\bar{1}$	<i>P</i> 2 ₁ / <i>c</i>	<i>P</i> 2 ₁ / <i>n</i>	<i>P</i> 1
<i>a</i> , Å	11.4866(8)	17.8209(10)	11.8600(3)	10.3592(2)
<i>b</i> , Å	14.6889(10)	10.1255(6)	21.6582(5)	10.4724(2)
<i>c</i> , Å	27.657(2)	23.1175(12)	19.9376(5)	11.3705(1)
α , deg	96.337(6)	90	90	102.787(1)
β , deg	90.484(6)	96.557(4)	101.649(1)	93.846(1)
γ , deg	102.217(5)	90	90	90.240(1)
<i>V</i> , Å ³	4530.4(6)	4144.2(4)	5015.8(2)	1200.00(3)
<i>T</i> , K	88(2)	90(2)	89(2)	84(2)
<i>Z</i>	4	4	4	1
Density (calcd), g cm ⁻³	1.64	1.56	1.63	1.61
<i>F</i> (000)	2240	1952	2472	584
μ , mm ⁻¹	3.25	3.49	3.05	3.07
Crystal size, mm ³	0.15 × 0.10 × 0.05	0.24 × 0.08 × 0.005	0.28 × 0.14 × 0.08	0.30 × 0.18 × 0.10
2 θ (min, max), deg	0.74, 27.98	1.77, 27.98	1.40, 27.88	1.99, 26.34
Number of reflections (collected)	75673	66483	63733	11614
Number of reflections (independent)	21545	9909	11847	8877
<i>T</i> (min, max)	0.5323, 0.8543	0.689, 0.983	0.4824, 0.7926	0.5475, 0.6683
Goodness of fit on <i>F</i> ²	1.01	0.97	1.01	1.06
R1, wR2 (observed data) ^a	0.0907, 0.1925	0.0791, 0.1388	0.0303, 0.0615	0.0623, 0.1520
R1, wR2 (all data)	0.2261, 0.2505	0.2008, 0.1816	0.0492, 0.0688	0.0640, 0.1542

$$^a R1 = \sum |F_o| - |F_c| / \sum |F_o|; wR2 = \{ \sum [w(F_o^2 - F_c^2)^2] / \sum [w(F_o^2)^2] \}^{1/2}.$$

dichloromethane/ethanol to give pure **8** (118 mg, 69%). Anal. Calcd for C₄₄H₃₈O₂OsP₂S: C, 59.85; H, 4.34. Found: C, 59.65; H, 4.54%. MS (*m/z*, ES+): calcd for C₄₄H₃₇O₂¹⁹²OsP₂S [M - H]⁺, 883.1599; found, 883.1599. IR (cm⁻¹): 2007(s) ν (CO), 1934(s) ν (CO). ¹H NMR (CDCl₃, δ): 7.62–7.26 (m, 30H, PPh₃); 7.08 (dm, ³J_{HH} = 12.0 Hz, 1H, H5); 6.08 (dm, ³J_{HH} = 12.0 Hz, 1H, H4); 4.44 (m, 1H, H2); 2.01 (m, 2H, H3); 1.55 (s, 3H, SCH₃). ¹³C NMR (CDCl₃, δ): 183.83 (t, ²J_{CP} = 8.4 Hz, CO); 181.97 (t, ²J_{CP} = 6.5 Hz, CO); 134.26 (t', ^{3,5}J_{CP} = 10.2 Hz, *m*-PPh₃); 132.97 (t', ^{1,3}J_{CP} = 51.4 Hz, *i*-PPh₃); 132.88 (t, ²J_{CP} = 12.0 Hz, *Cl*); 130.75 (t, ³J_{CP} = 5.1 Hz, *C*4); 129.53 (s, *p*-PPh₃); 127.17 (t', ^{2,4}J_{CP} = 9.8 Hz, *o*-PPh₃); 123.35 (t, ²J_{CP} = 13.6 Hz, *C*5); 118.69 (t, ³J_{CP} = 3.9 Hz, *C*2); 38.85 (t, ⁴J_{CP} = 3.0 Hz, *C*3); 18.32 (s, SCH₃). ³¹P NMR (CDCl₃, δ): -3.10 (s).

Synthesis of Os(C₅H₃{SMe-1}{H-3}{Me-3})(CO)₂(PPh₃)₂ (9**).** A solution of **2** (200 mg, 0.194 mmol) in THF (10 mL) was cooled to -78 °C. MeLi (300 μ L of a 1.6 M solution in Et₂O, 0.49 mmol) was slowly added, and the red color faded to pale tan. The mixture was allowed to warm to room temperature, and then all of the solvent was removed under reduced pressure. The resulting crude solid was recrystallized from dichloromethane/ethanol to give pure **9** as an off-white solid (104 mg, 60%). Anal. Calcd for C₄₅H₄₀O₂OsP₂S·CH₂Cl₂: C, 56.26; H, 4.31. Found: C, 56.34; H, 4.24 (¹H NMR spectrum shows presence of *ca.* 1 mol equiv of CH₂Cl₂ in the analytical sample). MS (*m/z*, ES+): calcd for C₄₅H₃₉O₂¹⁹²OsP₂S [M - H]⁺, 897.1755; found, 897.1737. IR (cm⁻¹): 1998 ν (CO) (s), 1930 ν (CO) (s). ¹H NMR (CDCl₃, δ): 7.57–7.28 (m, 30H, PPh₃); 7.10 (bd, ³J_{HH} = 11.7 Hz, 1H, H4); 5.96 (dm, ³J_{HH} = 11.9 Hz, 1H, H5); 4.61 (s, 1H, H2); 1.75 (m, 1H, H3); 1.69 (s, 3H, SCH₃); 0.42 (d, ³J_{HH} = 7.5 Hz, 3H, CH₃). ¹³C NMR (CDCl₃, δ): 183.95 (apparent t, ²J_{CP} = 8.6 Hz, CO); 182.27 (apparent t, ²J_{CP} = 6.7 Hz, CO); 138.58 (apparent t, ³J_{CP} = 4.9 Hz, *C*4); 134.50 (m, *m*-PPh₃); 134.11 (apparent t, ²J_{CP} = 12.1 Hz, *Cl*); 133.27 (dd, ¹J_{CP} = 12.8 Hz, ³J_{CP} = 5.3 Hz, *i*-PPh₃); 132.76 (dd, ¹J_{CP} = 12.8 Hz, ³J_{CP} = 5.3 Hz, *i*-PPh₃); 129.75 (bs, *p*-PPh₃); 129.68

(bs, *p*-PPh₃); 127.39 (d, ²J_{CP} = 2.2 Hz, *o*-PPh₃); 127.29 (d, ²J_{CP} = 2.2 Hz, *o*-PPh₃); 125.91 (apparent t, ³J_{CP} = 4.2 Hz, *C*2); 125.16 (apparent t, ²J_{CP} = 13.2 Hz, *C*5); 41.36 (apparent t, ⁴J_{CP} = 2.6 Hz, *C*3); 22.19 (apparent t, ⁵J_{CP} = 4.5 Hz, CH₃); 18.50 (s, SCH₃). ³¹P NMR (CDCl₃, δ): -3.51(*wk*), -5.86(*st*), -6.29(*st*), -8.64(*wk*).

Synthesis of [Os(C₅H₃{SMe-1}{Me-3})(CO)₂(PPh₃)₂Cl] (10**).** **9** (200 mg, 0.223 mmol) was added to a Schlenk tube and degassed dichloromethane (10 mL), and the resulting solution was frozen. CuCl₂ (36 mg, 0.27 mmol) was added to the frozen solution. The Schlenk tube was evacuated, and the mixture was warmed to room temperature. The solvent was removed under vacuum from the resulting purple solution. CHCl₃ was added to the resulting solid, and the solution was filtered to remove any excess copper salts. The solvent was then removed under vacuum, and the resulting purple solid was purified by column chromatography on alumina using dichloromethane as eluent. The purple band was collected, and the solvent was removed under reduced pressure to give pure **10** as purple crystals (100 mg, 48%). Anal. Calcd for C₄₅H₃₉ClO₂OsP₂S·CH₂Cl₂: C, 54.36; H, 4.07. Found: C, 54.44; H, 4.00 (¹H NMR spectrum shows presence of *ca.* 1 mol equiv of CH₂Cl₂ in the analytical sample). MS (*m/z*, ES+): calcd for C₄₅H₃₉O₂¹⁹²OsP₂S [M - Cl]⁺, 897.1755; found, 897.1726. IR (cm⁻¹): 2031(s) ν (CO), 1969(s) ν (CO). ¹H NMR (CDCl₃, δ): 10.86 (d, ²J_{CP} = 11.6 Hz, 1H, H5); 7.49–7.26 (m, 30H, PPh₃); 6.97 (d, ³J_{HH} = 11.5 Hz, 1H, H4); 5.89 (s, H2); 2.14 (s, 3H, SCH₃); 1.74 (s, 3H, CH₃). ¹³C NMR (CDCl₃, δ): 245.91 (t, ²J_{CP} = 6.8 Hz, *Cl*); 197.04 (t, ²J_{CP} = 10.6 Hz, *C*5); 181.58 (t, ²J_{CP} = 9.4 Hz, *C*4); 179.60 (t, ²J_{CP} = 7.8 Hz, *C*2); 171.28 (s, *C*3); 134.89 (bs, *C*4); 133.35 (t', ^{3,5}J_{CP} = 10.1 Hz, *m*-PPh₃); 131.53 (s, *p*-PPh₃); 129.69 (t', ^{1,3}J_{CP} = 56.0 Hz, *i*-PPh₃); 128.59 (t', ^{2,4}J_{CP} = 10.1 Hz, *o*-PPh₃); 126.15 (s, *C*2); 27.98 (s, CH₃); 24.60 (s, SCH₃). ³¹P NMR (CDCl₃, δ): 1.41 (s).

X-ray Crystal Structure Data. Single crystal X-ray measurements were made at *ca.* 90 K on a Bruker SMART APEX II

diffractometer with a CCD area detector using graphite-monochromatized Mo K α radiation ($\lambda = 0.71073 \text{ \AA}$). The crystals used were of different shapes with sizes of about 0.30 to 0.005 mm. Intensity data of all reflections were measured within the 2θ range of 1° – 30° . Data were integrated and corrected for Lorentz and polarization effects using SAINT.³⁹ Semiempirical absorption corrections were applied based on equivalent reflections using SADABS.⁴⁰ The structure solution and refinements were performed with the SHELXTL program package.⁴¹ Diagrams were produced using ORTEP3.⁴² A summary of the X-ray crystal structure data for **1**, **3**, **6**, and **7** is provided below in Table 2.

Computational Details. Using the Gaussian 03 program,⁴³ full geometry optimizations of the N electron iridabenzene **1** and the osmabenzenes Os(C₅H₄{SMe-1})I(CO)(PPh₃)₂ and **2** were carried out at the B3LYP level using the LANL2DZ basis sets for atoms Ir, Os, and I and 6-31(d) basis sets for all other atoms. NBO atomic charges were obtained for the N , $N - 1$, and $N + 1$ complexes (with the calculations for the $N - 1$ and $N + 1$ species being performed at the optimized geometry of the N electron complex) from single-point calculations at the B3LYP level using the LANL2DZ basis sets for atoms Ir, Os, and I and 6-311+(2d,p) basis sets for all other atoms. The condensed Fukui functions were obtained according to the eqs 1 and 2 ($f_k^- = q_k(N) - q_k(N - 1)$ (eq 1); $f_k^+ = q_k(N + 1) - q_k(N)$ (eq 2)) where q_k are the atomic charges at the k th atomic site and where $q_k(N)$, $q_k(N + 1)$, and

$q_k(N - 1)$ are the electron populations on atom k for the N , $N + 1$, and $N - 1$ electron species.^{35,36,44}

NBO atomic charges (and for comparison Mulliken charges) were used in the calculation of f_k^- and f_k^+ . Much closer agreement with experimental findings was obtained using the NBO charges as opposed to the Mulliken charges. The values derived from Mulliken charges are included in the Supporting Information. The whole molecules were used in the calculations because in a preliminary study we found that replacing PPh₃ with the model ligand PH₃ in these compounds gave significantly different results that were less consistent with the observations.

Acknowledgment. We thank the University of Auckland for support of this work through grants-in-aid and for access to the Computational Chemistry Group facilities. We also thank Mr. P. M. Johns for assistance with the calculations and production of the orbital diagram and Professor W. R. Roper for valuable discussions and comments.

Supporting Information Available: For compounds **1**, **2**, and **11**, coordinates of optimized geometries and Fukui functions for all atoms. Complete ref 43. Crystal and refinement data in CIF format for compounds **1**, **3**, **6**, and **7**. This material is available free of charge via the Internet at <http://pubs.acs.org>. Crystallographic data have been deposited with the Cambridge Crystallographic Data Centre (Fax: +44-1223-336-033; e-mail: deposit@ccdc.cam.ac.uk or <http://www.ccdc.cam.ac.uk>) as supplementary publication nos. CCDC 780439–780442 respectively.

JA105239T

(39) SAINT, *Area detector integration software*; Siemens Analytical Instruments Inc.: Madison, WI, 1995.

(40) Sheldrick, G. M. *SADABS, Program for semi-empirical absorption correction*; University of Göttingen: Göttingen, Germany, 1997.

(41) Sheldrick, G. M. *SHELXTL*; Siemens Analytical X-ray Systems: Madison, Wisconsin, USA.

(42) Burnett, M. N.; Johnson, C. K. *ORTEP-III: Oak Ridge Thermal Ellipsoid Plot Program for Crystal Structure Illustrations*; Oak Ridge National Laboratory Report ORNL-6895; 1996.

(43) Frisch, M. J.; et al. *Gaussian 03*, revision E.01; Gaussian Inc.: Wallingford, CT, 2004.

(44) Lewars, E. G. *Computational chemistry. Introduction to the theory and applications of molecular and quantum mechanics*; Kluwer Academic Publishers: Secaucus, NJ, 2003.